



Contents lists available at ScienceDirect

Tetrahedron

journal homepage: www.elsevier.com/locate/tet

A new “naked-eye” colorimetric and ratiometric fluorescent sensor for imaging Hg²⁺ in living cells

Pengcheng Yin, Qingfen Niu*, Qingxin Yang, Linxin Lan, Tianduo Li

Shandong Provincial Key Laboratory of Molecular Engineering, School of Chemistry and Pharmaceutical Engineering, Qilu University of Technology (Shandong Academy of Sciences), Jinan 250353, People's Republic of China

ARTICLE INFO

Article history:

Received 13 August 2019
Received in revised form
7 October 2019
Accepted 12 October 2019
Available online xxx

Keywords:

Ratiometric fluorescent sensor
Colorimetric
ICT
Hg²⁺
Cell imaging

ABSTRACT

A new oligothiophene-based sensor **3TH** for monitoring Hg²⁺ has been designed and synthesized based on the intramolecular charge transfer (ICT) mechanism. The **3TH** shows the significant specificity toward Hg²⁺ through “naked-eye” colorimetric detection as well as via ratiometric fluorescence enhancement response with low detection limit of 62 nM. In addition, sensor **3TH** shows high selectivity and sensitivity for Hg²⁺ with fast response in a suitable pH range. Moreover, the **3TH**-based test strips was used to conveniently detect Hg²⁺ ions in water. Furthermore, considering its good “turn-on” fluorescent sensing behavior and low cell cytotoxicity, **3TH** was successfully applied to detect and image Hg²⁺ in real water samples and living cells, which shows great potentials for application in environmental and biological systems.

© 2019 Elsevier Ltd. All rights reserved.

1. Introduction

Toxic effects of metal ions on physiological and pathological processes in living systems have recently attracted considerable research interest, which is considered as one of the forefront research areas in chemistry, biology and medicine [1]. Among the various metal ions, Hg²⁺ is considered as one of the most hazardous heavy metal ions, which can cause severe damages such as kidney failure, liver failure, DNA lesion, cognitive and motor disorders even in a very low concentration [2–7]. Due to its high toxicity and it can lead to serious environmental pollution and health hazard, therefore, building up a convenient, rapid and efficient method for detecting Hg²⁺ is extremely essential.

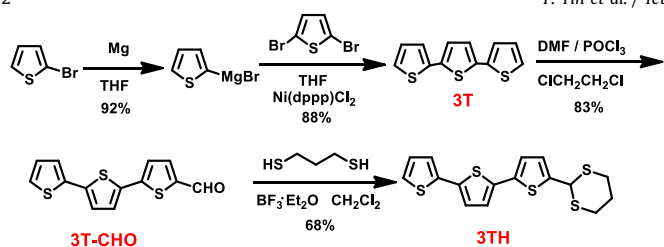
Apart from the traditional detection techniques, fluorescent sensor as a well-grounded method for detection of various analytes are of growing interest due to its outstanding advantages of great capability of temporal and spatial sampling, high sensitivity, and simple sample pretreatment [8–42]. However, in most practical applications, “turn-on”/“turn-off” type fluorescent sensor is based on the single fluorescence intensity change signal, and is generally influenced by the excitation intensity, sensor concentration,

photobleaching, and environment around the sensor (pH, polarity, and temperature etc) and stability under illumination, etc [43–48]. In order to eliminate the above-mentioned effects, ratiometric fluorescent sensor is exceptionally useful and is more attractive, which utilizes the ratio of the fluorescence intensity at two different wavelengths, and it also provides built-in correction for environmental factors and provide more accurate and precise measurement results with high sensitivity and inherent reliability [49–52]. To further application in the biological, food and environmental fields, the new ratiometric fluorescent sensor based on the intramolecular charge transfer (ICT) mechanism has recently received great research interest because of its unique ratiometric fluorescence behavior.

In this work, we reported the synthesis of a new thioacetal derivative of thioacetalized oligothiophene **3TH** (Scheme 1) and investigated its sensing behavior toward Hg²⁺. The investigated results indicated that the **3TH** shows highly selective, sensitive, “naked-eye” colorimetric and ratiometric fluorescent turn-on detection of Hg²⁺ in aqueous media based on the ICT mechanism. An obvious ICT process from oligothiophene moiety to aldehyde group causes a significant red-shift of the fluorescence band of the **3TH**, and produces a remarkable ratiometric fluorescent turn-on signal. The **3TH** shows very fast response towards Hg²⁺ with a quite low detection limit of 62 nM. More importantly, the sensor **3TH** was successfully applied to image Hg²⁺ ions in living cells.

* Corresponding author.

E-mail address: qf_niu1216@qlu.edu.cn (Q. Niu).

Scheme 1. The synthetic route of sensor **3TH**.

2. Experiment procedure

2.1. Reagents, materials and apparatus

All reagents were purchased from Sigma-Aldrich Chemical Company and used without further purification. Deionized water was used throughout all experiments. NMR spectra were recorded on a Bruker–AVANCE 400 NMR Spectrometer, with tetramethylsilane (TMS) as an internal standard. FTIR spectra were performed on Bruker ALPHA FT-IR spectrometer using KBr pellets. High resolution mass spectra (HRMS) were measured on an Agilent 6510 Accurate–Mass Q–TOF LC/MS system. Absorption and fluorescence spectra were measured on Shimadzu UV-2600 and Hitachi F-4600 spectrofluorometer, respectively. The pH measurements were performed on a Model PHS-3C pH meter. The cell fluorescence images were detected by a Leica TCS SP8 confocal-laser scanning microscope (CL SM) with an objective oil lens of 63X magnification.

2.2. General procedure for the spectra measurement

3TH was dissolved in ethanol to prepare the 1.0 mM of stock solution. The appropriate amount of each inorganic metallic salts (K^+ , Na^+ , Ag^+ , Ca^{2+} , Mg^{2+} , Ba^{2+} , Al^{3+} , Co^{2+} , Cu^{2+} , Ni^{2+} , Pb^{2+} , Hg^{2+} , Zn^{2+} , Cd^{2+} , Cr^{3+} , Sr^{2+} , Fe^{2+} , and Fe^{3+}) was dissolved in deionized water at a concentration of 1.0 mM. Test solutions were prepared by placing the stock solutions and diluted to the desired analytical concentrations with a mixed solution of EtOH/H₂O (1/1, v/v). All measurements were carried out at room temperature, the excitation wavelength was 360 nm with excitation and emission slit widths of 5 and 5 nm, respectively.

2.3. Synthesis of sensor **3TH**

Compound **3T-CHO** (50 mg, 0.18 mmol) and 1,3-malonolthiol (39 mg, 0.36 mmol) were dissolved in dry dichloromethane (10 mL), a catalytic amount of $BF_3 \cdot Et_2O$ (0.02 mL, 0.15 mmol) as the Lewis acid added into the above solution. The reaction mixture was stirred at room temperature for 10 h under an atmosphere of argon. Then, the reaction mixture was evaporated in vacuo, and the crude product was purified by column chromatography to obtain compound **3TH**, which is as a yellow solid (45 mg, 68% yield). Mp 136.8–137.5 °C; FTIR (KBr, cm^{-1}) $\nu = 1059$ (C–S–C), 1503 (C=C, thiophene ring); 1H NMR (400 Hz, DMSO- d_6 , ppm): $\delta = 7.53$ (d, $J = 4.8$ Hz, 1H), 7.34 (d, $J = 3.2$ Hz, 1H), 7.26 (s, 2H), 7.18 (d, $J = 3.6$ Hz, 1H), 7.09 (m, $J = 8.8$ Hz, 2H), 5.73 (s, 1H), 3.05 (t, $J = 11.6$ Hz, 2H), 2.89 (d, $J = 14$ Hz, 2H), 2.08 (d, $J = 14$ Hz, 1H), 1.76 (d, $J = 14$ Hz, 1H); ^{13}C NMR (100 Hz, DMSO- d_6 , ppm): $\delta = 142.2$, 135.9, 135.8, 135.6, 134.8, 128.4, 127.2, 125.7, 125.1, 124.9, 124.3, 123.6, 79.6, 43.4, 30.1, 24.6; HRMS (ESI) m/z calcd for $C_{16}H_{14}S_5 [M+H]^+$: 369.9777; Found 366.9782.

2.4. Fluorescence imaging of Hg^{2+} in living cells

The HeLa cells were cultured in DMEM supplemented with 10% FBS at 37 °C (under 5% CO_2), which were chosen for the cell imaging experiments. Firstly, the living HeLa cells and sensor **3TH** (10 μ M) were cultured in cell culture media for 1 h at 37 °C, washed with PBS buffer (pH = 7.4) for three times, and then imaging. Next, Hg^{2+} (10 μ M) was added to the pre-cultured cells of the **3TH**, cultured for 30 min at 37 °C, and washed with PBS for three times, then imaging. After 60 min, imaging the cells that loaded Hg^{2+} again were detected under CLSM. The excitation wavelength was 488 nm, and the emission filter was 500–550 nm.

3. Results and discussion

3.1. Design and synthesis of **3TH**

As described in Scheme 1, compound **3TH** was facilely synthesized from **3T-CHO** [53] and 1,3-malonolthiol. The structure of **3TH** was well confirmed by 1H NMR, ^{13}C NMR, FTIR and HRMS (Figs. S1–4). Our design strategy was based on the well-known Hg^{2+} -promoted desulfurization reaction of thioacetal to the corresponding aldehyde.

3.2. UV–vis spectral response of **3TH** to Hg^{2+}

Initially, the selectivity study of sensor **3TH** towards Hg^{2+} was evaluated. The UV–vis response of **3TH** (10 μ M) was carried out after addition of a series of 2.0 equiv. metal ions (K^+ , Na^+ , Ag^+ , Ca^{2+} , Mg^{2+} , Ba^{2+} , Al^{3+} , Co^{2+} , Cu^{2+} , Ni^{2+} , Pb^{2+} , Hg^{2+} , Zn^{2+} , Cd^{2+} , Cr^{3+} , Sr^{2+} , Fe^{2+} , and Fe^{3+}) in EtOH/H₂O (1:1, v/v) solution. As shown in Fig. 1, the **3TH** (10 μ M) exhibited a maximal absorption band at 360 nm, which should be ascribed to the absorption of oligothiophene moiety. Upon addition of various metal ions (2.0 equiv.), only Hg^{2+} induced great changes: a typical absorption at 360 nm reduced significantly while a new red-shift absorption band is created at 400 nm along with the solution color change from colorless to pale yellow. Whereas, other metal ions caused no significant color and spectral changes. These results indicated that the colorimetric sensor **3TH** has high selectivity towards Hg^{2+} .

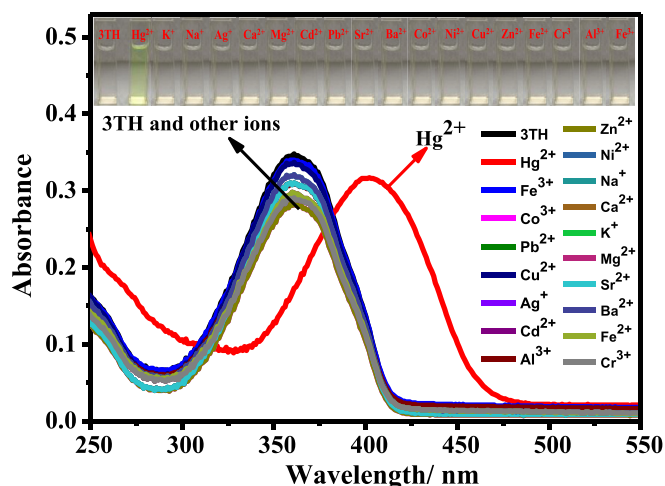


Fig. 1. The UV–vis absorption spectra of **3TH** (10 μ M) after addition of 2.0 equiv. of various metal ions in EtOH/H₂O (1/1, v/v) solution; **Inset**: Colorimetric responses of **3TH** (10 μ M) in an EtOH/H₂O (1:1, v/v) solution upon the addition of 2.0 equiv. of various metal ions.

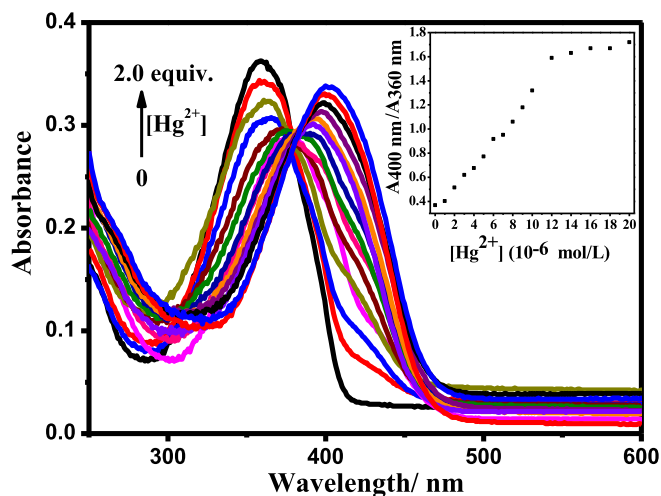


Fig. 2. The absorption spectra of **3TH** (10 μM) exposed to various concentrations of Hg^{2+} (0–2.0 equiv.) in EtOH/ H_2O (1/1, v/v) solution.

To insight into the colorimetric response of the **3TH** toward Hg^{2+} , the absorption spectra of **3TH** with various concentrations of Hg^{2+} (0–2.0 equiv.) in EtOH/ H_2O (1:1, v/v) solution were recorded. As displayed in Fig. 2, with increasing concentration of Hg^{2+} , the absorption intensity at 360 nm decreased gradually and the absorption band at 400 nm increased progressively. Meanwhile, the ratio (A_{400}/A_{360}) of the absorbance shows a gradual increase with the increased concentrations of Hg^{2+} , and reached saturation at 10 μM of Hg^{2+} . In addition, a clear well-formed isobestic point at 381 nm was clearly observed, suggesting the formation of a new species based on the Hg^{2+} -triggered deprotection reaction of **3TH**.

3.3. Ratiometric fluorescence response of **3TH** to Hg^{2+}

Next, the fluorescence response of **3TH** was examined with the above of metal ions (2.0 equiv.). As shown in Fig. 3, with the excitation at 360 nm, sensor **3TH** showed a blue emission centered

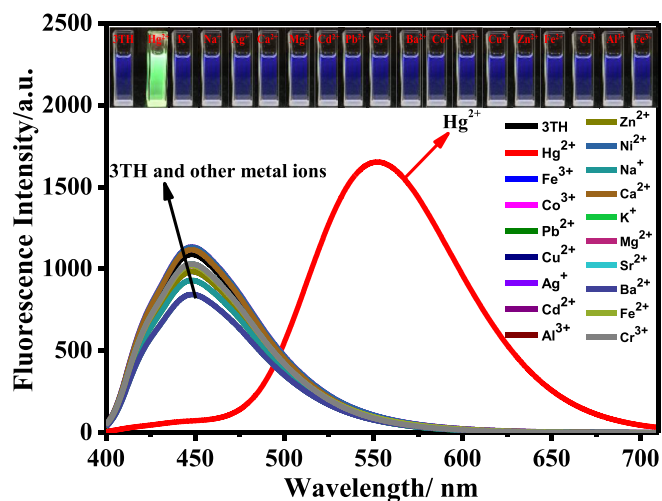


Fig. 3. Fluorescence spectra of **3TH** (10 μM) in the presence of various metal ions (2.0 equiv.) in EtOH/ H_2O (1/1, v/v) solution; **Inset**: Fluorimetric responses of **3TH** (10 μM) in an EtOH/ H_2O (1:1, v/v) solution upon the addition of 2.0 equiv. of various metal ions.

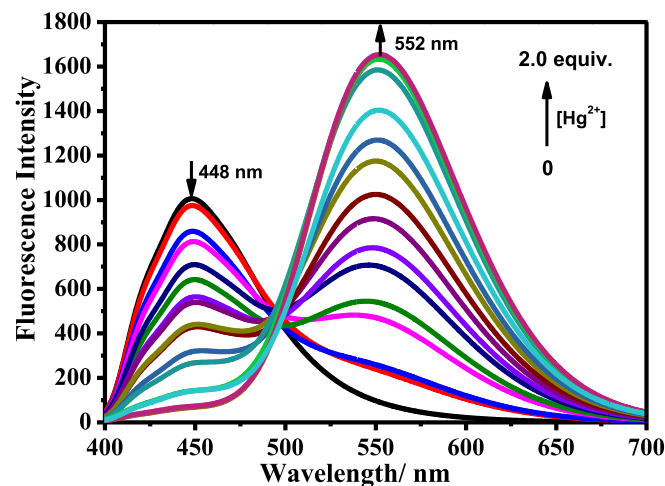


Fig. 4. Fluorescence titration spectra of **3TH** (10 μM) with different concentrations of Hg^{2+} (0–2.0 equiv.) in EtOH/ H_2O (1/1, v/v) solution.

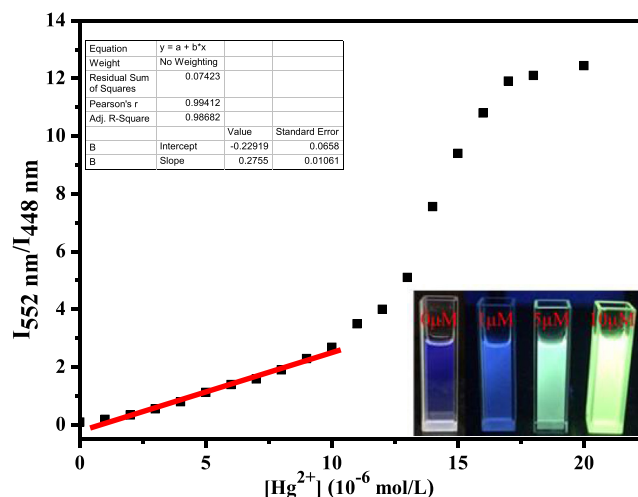


Fig. 5. Fluorescence intensity ratio (I_{552}/I_{448}) of sensor **3TH** upon gradual addition of Hg^{2+} (0–2.0 equiv.); **insets**: Fluorescence photographs of sensor **3TH** in the presence of different concentration of Hg^{2+} .

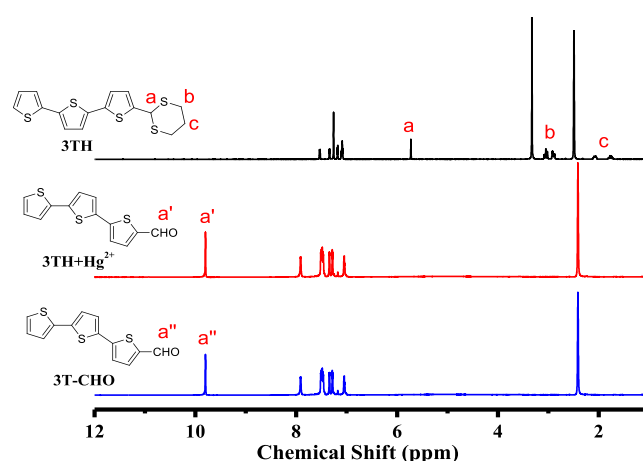
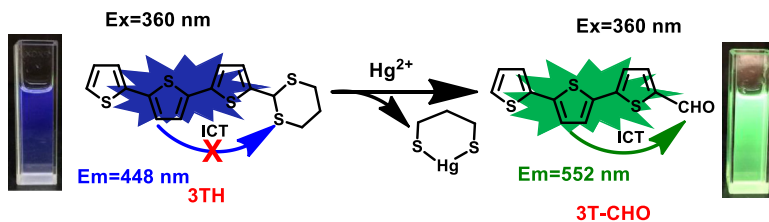


Fig. 6. ^1H NMR spectra of **3TH**, **3TH** upon the addition of 1.0 equiv. Hg^{2+} (**3TH** + Hg^{2+}) and **3T-CHO** in $\text{DMSO-}d_6$.



Scheme 2. Proposed complexation model of **3TH** with Hg^{2+} and the observed colorimetric change.

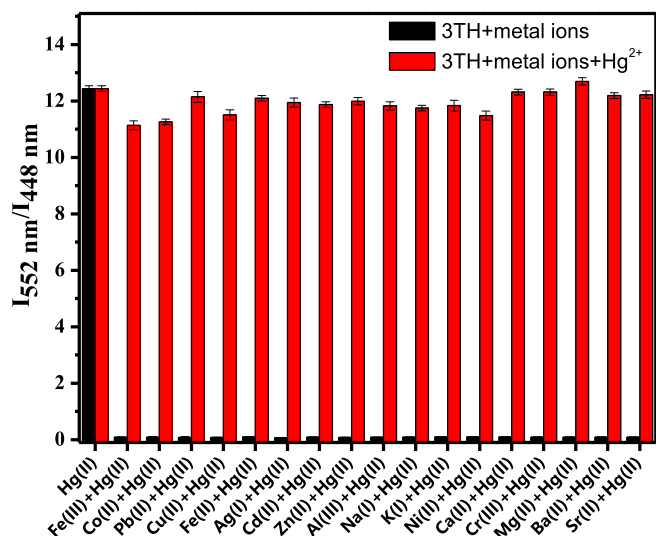


Fig. 7. Fluorescence intensity ratio (I_{552}/I_{448}) of **3TH** ($10\ \mu\text{M}$) exposed to 2.0 equiv various metal ions and to the mixture of 2.0 equiv. Hg^{2+} in EtOH/ H_2O (1/1, v/v) solution.

about 448 nm. With the addition of metal ions except for Hg^{2+} to **3TH** in EtOH/ H_2O (1:1, v/v) solution, almost no spectral and solution color changes were observed. Fascinatingly, the addition of Hg^{2+} to sensor **3TH** resulted in a considerable enhancement of

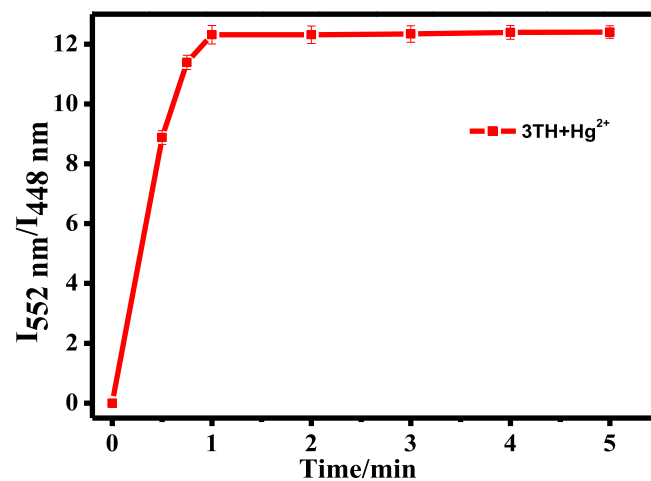


Fig. 9. Time-dependent of the fluorescence intensity ratios (I_{552}/I_{448}) of **3TH** ($10\ \mu\text{M}$) upon addition of 2.0 equiv Hg^{2+} in EtOH/ H_2O (1/1, v/v) solution.

fluorescence intensity at 552 nm via fluorescence turn-on response and a significant decrease of fluorescence intensity at 448 nm, along with the solution color change from blue to bright green under 365 nm lamp. The result revealed that **3TH** can function as a fluorescent turn-on sensor for highly selective detection of Hg^{2+} .

To examine the sensitivity of **3TH** for Hg^{2+} sensing, the fluorescence titration of **3TH** ($10\ \mu\text{M}$) with Hg^{2+} (0–2.0 equiv.) was performed as shown in Fig. 4. With increasing of concentration of Hg^{2+} , a gradual decrease of the emission peak occurred at 448 nm and a progressive increase of new red-shift emission band at 552 nm along with a distinct isoemission point at 495 nm, which gives measurable ratiometric fluorescent signals. The emission intensity ratios at 552 nm and 448 nm (I_{552}/I_{448}) underwent a remarkable change with 13-fold emission enhancement with increasing Hg^{2+} and reached the platform at $10\ \mu\text{M}$ (Fig. 5). The large red-shift (104 nm) and the distinct ratiometric fluorescent enhancement signals in **3TH** were due to electron-rich dithioacetal moiety which could be removed by Hg^{2+} to release the electron-deficient aldehyde group, and produced strong push-pull electronic system, leading to the ICT process from oligothiophene moiety to aldehyde group switched on. A preferable linearity ($R^2 = 0.98686$) between the $[\text{Hg}^{2+}]$ and emission ratios (I_{552}/I_{448}) was clearly observed along with sensitive solution color changes from blue to green (Fig. 5), indicating that **3TH** was a Hg^{2+} -specific ratiometric fluorescent turn-on sensor for quantitatively and qualitatively detecting Hg^{2+} . The detection limit of **3TH** was determined to be 62 nM ($\text{LOD} = 3\sigma/k$), which is lower than those of most reported ratiometric fluorescent sensors previously [54–56], further indicating **3TH** has high sensitivity to Hg^{2+} .

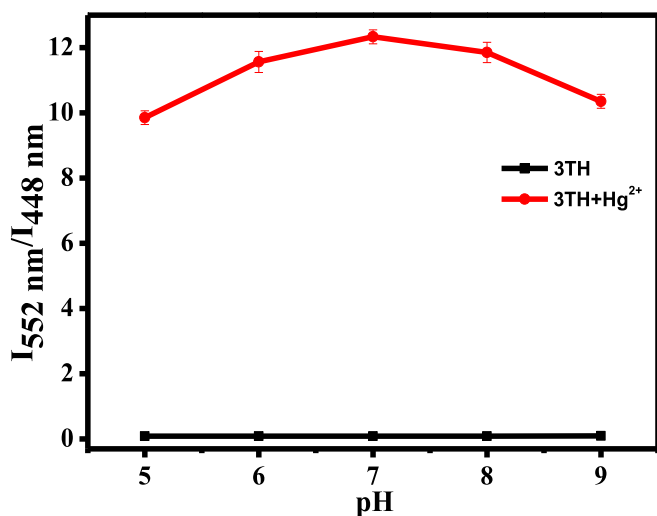


Fig. 8. Fluorescence intensity ratio (I_{552}/I_{448}) of sensor **3TH** ($10\ \mu\text{M}$) at various pH values in an EtOH/ H_2O solution (1/1, v/v) in the absence and presence of Hg^{2+} (2.0 equiv.) at room temperature.

Table 1
Determination of Hg²⁺ in environmental water samples by the proposed method.

Sample	Added (μM)	Detect ($x \pm \text{SD}$) (μM)	Recovery (%)	Relative error (%)	RSD (%)
Tap water	5.0	4.87 \pm 0.14	97.4	2.6	2.8
	10.0	10.22 \pm 0.19	102.2	2.2	1.8
River water	5.0	5.13 \pm 0.11	102.6	2.6	2.1
	10.0	9.77 \pm 0.29	97.7	2.3	2.9
Distilled Water	5.0	4.85 \pm 0.13	97.0	3.0	2.6
	10.0	10.31 \pm 0.14	103.1	3.1	1.4
The Yellow River	5.0	4.89 \pm 0.11	97.8	2.2	2.2
	10.0	10.33 \pm 0.34	103.3	3.3	3.3
Lake Water of Ji'nan Garden Expo	5.0	5.14 \pm 0.15	102.8	2.8	2.9
	10.0	10.32 \pm 0.10	103.2	3.2	0.9

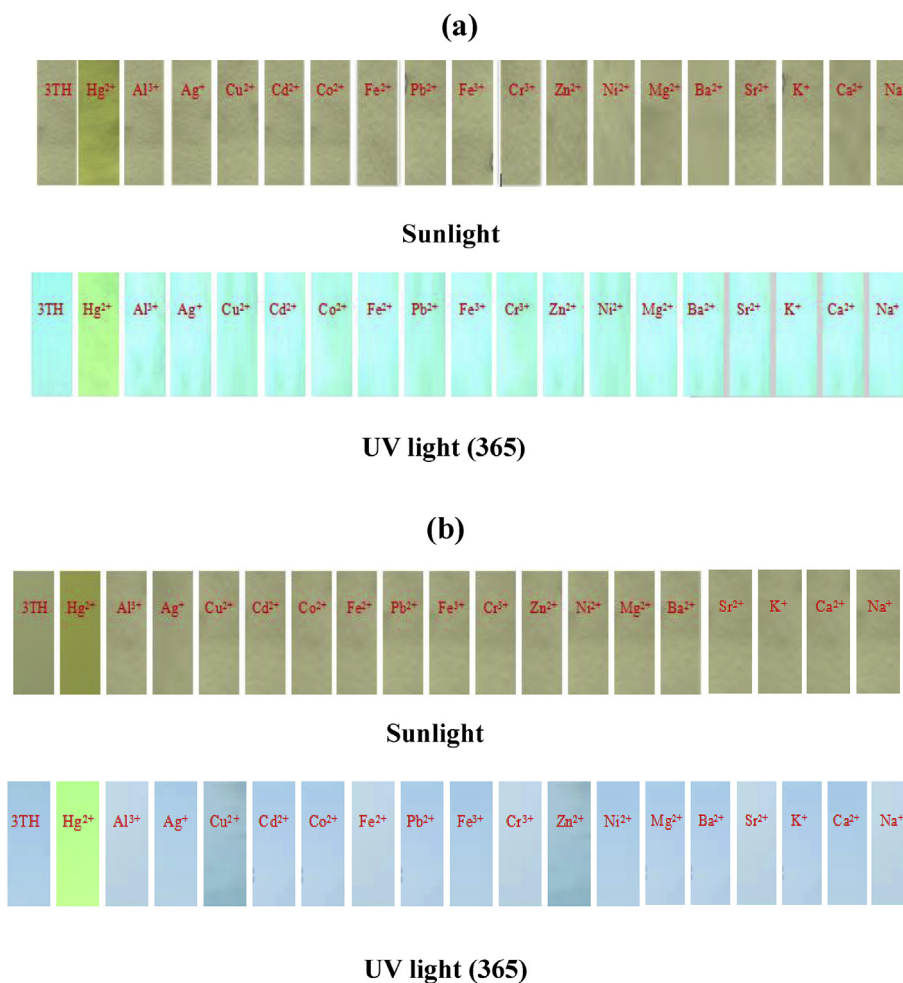


Fig. 10. Photographs showing the color changes of sensor **3TH** before and after addition of Hg²⁺ and other ions on filter papers (a) and TLC plates (b).

3.4. Reaction mechanism studies

To study the reaction mechanism, ¹H NMR titration was firstly carried out. As shown in Fig. 6, upon the addition of Hg²⁺ (1.0 equiv.) into **3TH** (10 μM) in DMSO-*d*₆, the characteristic 1,3-dithiane methine proton signal at 5.73 ppm disappeared with a concomitant appearance of a new proton signal at 9.80 ppm, which assigned to the corresponding aldehyde proton of **3T-CHO**. The ¹H NMR spectrum of **3TH** + Hg²⁺ was well identical to that of **3T-CHO**, further proved the production of **3T-CHO** from the reaction between **3TH** and Hg²⁺. Then, the reaction product of **3TH** with Hg²⁺ has been further confirmed by FTIR spectra (Fig. S5). The FTIR

spectra shows a new typical and prominent absorption peak of aldehyde group at 1650 cm⁻¹ in the presence of Hg²⁺ (1.0 equiv), which is similar to that of **3T-CHO**, giving another proof that the resulting product is essentially identical to that of **3T-CHO**. In addition, upon the addition of Hg²⁺ to the sensor, the optical spectra of **3TH** along with the distinct color changes are the same as that of **3T-CHO** (Figs. S6 and S7), further demonstrating that **3TH** was indeed converted into **3T-CHO** by Hg²⁺. Based on these investigated results, the reaction mechanism between **3TH** with Hg²⁺ occurs as shown in Scheme 2, the **3TH** for selectively sensing of Hg²⁺ is based on the Hg²⁺-triggered deprotection reaction of oligothiophene thioacetals [57–61], which resulted in the ICT on

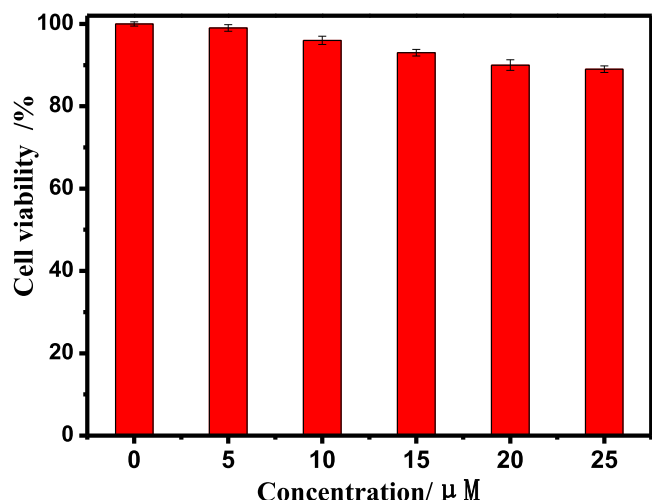


Fig. 11. Cellular activity of **3TH** against HeLa cells at different concentrations (0–25 μM).

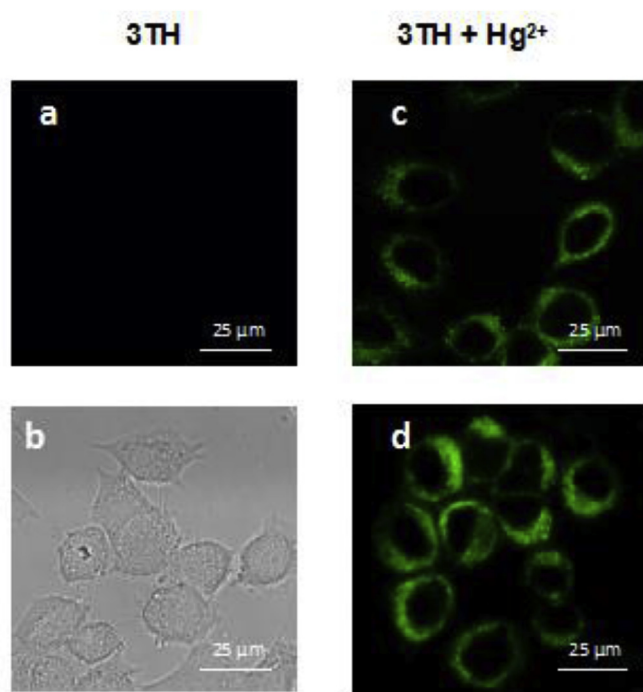


Fig. 12. Confocal microscopy images of HeLa cells. (a) Fluorescent image of HeLa cells with **3TH** for 1 h; (b) Bright-field image of HeLa cells with **3TH** for 1 h; (c) Fluorescent images of HeLa cells incubated with **3TH** and Hg^{2+} for 30 min; (d) for 60 min.

and thus caused a large red-shift and distinct ratiometric fluorescence enhancement in emission spectra.

3.5. Competition studies

To check the high selectivity of sensor **3TH** sensing response to Hg^{2+} , the competition experiments were carried out in the presence of Hg^{2+} ions (2.0 equiv.) mixed with other relevant tested metal ions (2.0 equiv.) in EtOH/ H_2O (1:1, v/v) solution. As shown in Fig. 7, there was no significant variation on the Hg^{2+} -induced emission ratiometric signal (I_{552}/I_{448}) of **3TH** for detection of Hg^{2+} mixed

with other competitive metal ions. The investigation suggests that **3TH** behaves as a highly selective ratiometric fluorescent turn-on sensor for Hg^{2+} and is quite useful for selectively detecting Hg^{2+} in environmental and biological systems.

3.6. Effect of pH

To ensure that the sensor **3TH** is suitable for detecting Hg^{2+} under a physiological pH range, the pH-dependent experiment with different pH values was recorded in EtOH/ H_2O (1:1, v/v) solution (Fig. 8). It is found that no dramatic change in the fluorescence ratios (I_{552}/I_{448}) of **3TH** during the pH range 5.0–9.0. By treatment with Hg^{2+} (2.0 equiv.), from pH 5.0 to 7.0, the fluorescence ratios (I_{552}/I_{448}) showed a gradual increase, while it showed a decreasing trend from pH 7.0 to 9.0, which may be due to hydrolysis of Hg^{2+} at pH 7.0–9.0. The proposed ratiometric fluorescent sensor **3TH** is applicable in a wide range of pH (5.0–9.0), which indicates that it can monitor Hg^{2+} under physiological pH conditions.

3.7. Reaction time on sensing Hg^{2+}

A short response time is a key factor for a designed sensor [62,63], therefore, the time dependent fluorescence responses of **3TH** toward Hg^{2+} (2.0 equiv.) were investigated in EtOH/ H_2O (1:1, v/v) solution. As shown in Fig. 9, a dramatic enhancement in the emission ratios (I_{552}/I_{448}) was quickly detected, reached the maximum within 1 min, and then remained stable with increasing time. The result indicated that the fluorescence assay time of 1 min was selected in the evaluation of the selectivity and sensitivity of the **3TH** toward Hg^{2+} under mild conditions and without any catalyst.

3.8. Application of **3TH** to real water samples

To evaluate the applicability of the sensor **3TH** to real samples, water samples including tap water, river water, distilled water, the Yellow River, and lake water of Ji'nan Garden Expo were analyzed using a standard addition method. A series of various concentrations of Hg^{2+} are spiked in these test samples. As displayed in Table 1, the analytical results obtained from the water samples show satisfactory recoveries ranging between 97.8% and 103.3% with low relative standard deviation (RSD) below 3.3%. These determined values were in good agreement with the added values, confirming the applicability of the proposed sensor **3TH** in the environmental water samples with high sensitivity, good reliability and efficiency.

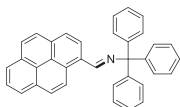
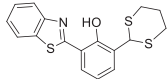
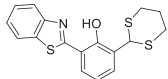
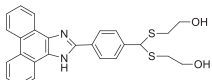
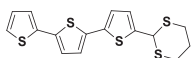
3.9. Sensor **3TH**-based test strips

Ease of applicability of a developed sensor is a performance index that makes it more convenient to use. To further investigate the practical application of sensor **3TH**, we prepared test strips by dipping filter paper/TLC plate into the EtOH solution of **3TH** (1.0 mM) and then dried in air. When these test strips coating **3TH** immersed into the solution of each metal ion (1.0 mM) in water, we found that only Hg^{2+} ions induced immediate and apparent color changes under sunlight and 365 nm UV lamp, respectively, other metal ions caused almost no change (Fig. 10). Therefore, these **3TH**-based test strips could be conveniently handled at any moment for the selective colorimetric detection of Hg^{2+} ions by the naked eyes.

3.10. Cellular imaging of Hg^{2+}

Inspired by the excellent “turn-on” fluorescent sensing behavior of sensor **3TH** for Hg^{2+} , the cellular imaging capability in living

Table 2
The comparisons of **3 TH** for Hg²⁺ with other Hg²⁺-sensitive sensors.

Compound	Sensing method	LOD (μM)	pH range	Test Strips	Response time	Cells Imaging	Ref.
	fluorescence turn-on	0.42	no data	no date	no date	yes	[64]
	fluorescence turn-on	3.20	3.0–10.0	no date	10 min	yes	[65]
	fluorescence turn-on	0.20	3.0–5.0	no date	no date	no date	[66]
	fluorescence turn-on	1.16	no data	no date	1 min	yes	[67]
	naked-eye colorimetric/ratiometric fluorescent turn-on	0.062	5.0–9.0	Yes	1 min	yes	This work

HeLa cells was further studied. Firstly, the cytotoxicity of **3 TH** towards HeLa cells at different concentrations (0–25 μM) were tested using MTT assay (Fig. 11). The tested result indicates that **3 TH** has low cytotoxicity to the living cells, because the cellular viability is nearly 90% over 24 h even at high concentration. Next, HeLa cell imaging experiments were measured with sensor **3 TH** at the concentration of 10 μM. Sensor **3 TH** incubation alone for 60 min gave no fluorescence in the related regions (Fig. 12a and b). Then, the HeLa cells were firstly incubated with **3 TH** for 30 min and washed off the excess sensors that did not enter the cells, then the Hg²⁺ were added and incubated for 30 min, significant green fluorescence was observed (Fig. 12c). As the incubation time prolonged to 60 min, a stronger green fluorescence was displayed in the cytoplasm (Fig. 12d). Therefore, these cell imaging results demonstrated that sensor **3 TH** can effectively image Hg²⁺ in living cells.

3.11. Comparison with other reported sensitive-Hg²⁺ sensors

Compared with other reported sensitive Hg²⁺ fluorescent sensors [64–67], and the analytical results were listed in Table 2. Our designed sensor **3 TH** showed some outstanding advantages including naked-eye colorimetric and ratiometric fluorescent turn-on detection, low detection limit, fast response, wide working pH range, and multifunctional applications in test strips, environmental water and live-cell imaging.

4. Conclusion

In summary, we developed a new oligothiophene-based sensor **3 TH** based on the ICT mechanism, which shows fast, “naked-eye” colorimetric and ratiometric fluorescent turn-on detection of Hg²⁺ in aqueous media. The low-cost sensor **3 TH** with low toxicity exhibited high sensitivity and superior selectivity toward Hg²⁺ in a favorable working pH range. Due to its excellent features, the sensor **3 TH** was successfully applied to detect and image Hg²⁺ in environmental water, test strips and living cells, which provided a convenient, reliable and accurate method for Hg²⁺ analysis.

Declaration of competing interest

The authors declared that they have no conflicts of interest to this work.

We declare that we do not have any commercial or associative interest that represents a conflict of interest in connection with the work submitted.

Acknowledgment

We are thankful for the financial support from the Natural Science Foundation of Shandong Province (No. ZR2017LB009), the National Natural Science Foundation of China (Nos. 21376125 and 21776143), the program for College Students' Innovation and Entrepreneurship Training of Shandong Province (No. S201910431035), and the Program for Scientific Research and the Program for Scientific Research Innovation Team in Colleges and Universities of Shandong Province (No. 0308150302).

Appendix A. Supplementary data

Supplementary data to this article can be found online at <https://doi.org/10.1016/j.tet.2019.130687>.

References

- [1] A. Tasleem, M. Azam, K. Siddiqui, A. Ali, I. Choi, Q. Mohd, R. Haq, *Int. J. Mol. Sci.* 16 (2015) 29592–29630.
- [2] A. Han, X. Liu, G.D. Prestwich, L. Zang, *Sens. Actuators B Chem.* 198 (2014) 274–277.
- [3] M. Vedamalai, D. Kedaria, R. Vasita, S. Moric, I. Gupta, *Dalton Trans.* 45 (2016) 2700–2708.
- [4] S.A. Counter, L.H. Buchanan, *Toxicol. Appl. Pharmacol.* 198 (2004) 209–230.
- [5] M. Gochfeld, *Ecotoxicol. Environ. Saf.* 56 (2003) 174–179.
- [6] C.M.L. Carvalho, E.H. Chew, S.I. Hashemy, J. Lu, A. Holmgren, *J. Biol. Chem.* 283 (2008) 11913–11923.
- [7] T.W. Clarkson, L. Magos, G.J. Myers, *N. Engl. J. Med.* 349 (2003) 1731–1737.
- [8] A.R. Lippert, E.J. New, C.J. Chang, *J. Am. Chem. Soc.* 133 (2011) 10078–10080.
- [9] H. Kobayashi, M. Ogawa, R. Alford, P.L. Choyke, Y. Urano, *Chem. Rev.* 110 (2010) 2620–2640.
- [10] H. Peng, Y. Cheng, C. Dai, A.L. King, B.L. Predmore, D.J. Lefer, B.A. Wang, *Angew. Chem. Int. Ed.* 50 (2011) 9672–9675.
- [11] X. Li, X. Gao, W. Shi, H. Ma, *Chem. Rev.* 114 (2014) 590–659.
- [12] X. Chen, F. Wang, J.Y. Hyun, T. Wei, J. Qiang, X. Ren, I. Shin, J. Yoon, *Chem. Soc. Rev.* 45 (2016) 2976–3016.
- [13] W. Xu, Z. Zeng, J.H. Jiang, Y.T. Chang, L. Yuan, *Angew. Chem. Int. Ed.* 55 (2016)

- 13658–13699.
- [14] L. He, B. Dong, Y. Liu, W. Lin, *Chem. Soc. Rev.* 45 (2016) 6449–6461.
- [15] V.S. Lin, W. Chen, M. Xian, C.J. Chang, *Chem. Soc. Rev.* 44 (2015) 4596–4618.
- [16] J. Yin, Y. Hua, J. Yoon, *Chem. Soc. Rev.* 44 (2015) 4619–4644.
- [17] S. Zhang, Q. Niu, L. Lan, *Sens. Actuators B Chem.* 240 (2017) 793–800.
- [18] Z. Guo, Q. Niu, T. Li, *Spectrochim. Acta A* 200 (2018) 76–84.
- [19] Q. Niu, X. Wu, S. Zhang, T. Li, Y. Cui, X. Li, *Spectrochim. Acta A* 153 (2016) 143–146.
- [20] Y. Li, Q. Niu, T. Wei, T. Li, *Anal. Chim. Acta* 1049 (2019) 196–212.
- [21] Q. Niu, T. Sun, T. Li, Z. Guo, H. Pang, *Sens. Actuators B Chem.* 266 (2018) 730–743.
- [22] Z. Guo, T. Hu, T. Sun, T. Li, H. Chi, Q. Niu, *Dyes Pigments* 163 (2019) 667–674.
- [23] Z. Guo, Q. Niu, Q. Yang, T. Li, H. Chi, *Anal. Chim. Acta* 1065 (2019) 113–123.
- [24] L. Lan, T. Li, T. Wei, H. Pang, T. Sun, E. Wang, H. Liu, Q. Niu, *Spectrochim. Acta A* 193 (2018) 289–296.
- [25] X. Wu, Q. Niu, T. Li, Y. Cui, S. Zhang, *J. Lumin.* 175 (2016) 182–186.
- [26] Q. Niu, L. Lan, T. Li, Z. Guo, T. Jiang, Z. Zhao, Z. Feng, J. Xi, *Sens. Actuators B Chem.* 276 (2018) 13–22.
- [30] T. Sun, Q. Niu, Y. Li, T. Li, T. Hu, E. Wang, H. Liu, *Sens. Actuators B Chem.* 258 (2018) 64–71.
- [31] Z. Guo, Q. Niu, T. Li, T. Sun, H. Chi, *Spectrochim. Acta A* 213 (2019) 97–103.
- [32] T. Sun, Y. Li, Q. Niu, T. Li, Y. Liu, *Spectrochim. Acta A* 195 (2018) 142–147.
- [33] T. Sun, Q. Niu, T. Li, Z. Guo, H. Liu, *Spectrochim. Acta A* 188 (2018) 411–417.
- [34] S. Zhang, T. Sun, D. Xiao, F. Yuan, T. Li, E. Wang, H. Liu, Q. Niu, *Spectrochim. Acta A* 189 (2018) 594–600.
- [35] Z. Zuo, X. Song, D. Guo, Z. Guo, Q. Niu, *J. Photochem. Photobiol., A* 382 (2019) 111876.
- [36] J. Wang, T. Wei, F. Ma, T. Li, Q. Niu, *J. Photochem. Photobiol., A* 383 (2019) 111982.
- [37] Z. Guo, T. Hu, X. Wang, T. Sun, T. Li, Q. Niu, *J. Photochem. Photobiol., A* 371 (2019) 50–58.
- [38] Z. Guo, Q. Niu, T. Li, E. Wang, *Tetrahedron* 75 (2019) 3982–3992.
- [39] J. Wang, Q. Niu, T. Hu, T. Li, T. Wei, *J. Photochem. Photobiol., A* 384 (2019) 112036.
- [40] R. Huang, X.L. Zheng, C.C. Wang, R.Y. Wu, S.Y. Yan, J.Q. Yuan, W.X. Cheng, X. Zhou, *Chem. Asian J.* 7 (2012) 915–918.
- [41] J.H. Bi, M.X. Fang, J.B. Wang, S. Xia, Y.B. Zhang, J.T. Zhang, G. Vegesan, S.W. Zhang, M. Tanasova, F.-T. Luo, H.Y. Liu, *Inorg. Chim. Acta* 468 (2017) 140–145.
- [42] M.X. Fang, S. Xia, J.H. Bi, T.P. Wigstrom, L. Valenzano, J.B. Wang, M. Tanasova, R.L. Luck, H.Y. Liu, *Molecules* 24 (2019) 1592–1602.
- [43] Y. Liu, K. Li, K.X. Xie, L.L. Li, K.K. Yu, X. Wang, X.Q. Yu, *Chem. Commun.* 52 (2016) 3430–3433.
- [44] M.H. Lee, B. Yoon, J.S. Kim, J.L. Sessler, *Chem. Sci.* 4 (2013) 4121–4126.
- [45] M.H. Lee, J.S. Kim, J.L. Sessler, *Chem. Soc. Rev.* 44 (2015) 4185–4191.
- [46] J. Fan, M. Hu, P. Zhan, X. Peng, *Chem. Soc. Rev.* 42 (2013) 29–43.
- [47] X. Jia, Q. Chen, Y. Yang, Y. Tang, R. Wang, Y. Xu, W. Zhu, X. Qian, *J. Am. Chem. Soc.* 138 (2016) 10778–10781.
- [48] K. Gu, Y. Xu, H. Li, Z. Guo, S. Zhu, S. Zhu, P. Shi, T.D. James, H. Tian, W.-H. Zhu, *J. Am. Chem. Soc.* 138 (2016) 5334–5340.
- [49] Y. Sun, D. Zhao, S. Fan, L. Duan, *Sens. Actuators B Chem.* 208 (2015) 512–517.
- [50] L. Cui, C. Ji, Z. Peng, L. Zhong, C. Zhou, L. Yan, S. Qu, S. Zhang, C. Huang, X. Qian, Y. Xu, *Anal. Chem.* 86 (2014) 4611–4617.
- [51] B. Zhu, C. Gao, Y.C. Zhao, Y. Li, Q. Wei, Z. Ma, B. Du, X. Zhang, *Chem. Commun.* 47 (2011) 8656–8658.
- [52] M.H. Lee, J.S. Kim, J.L. Sessler, *Chem. Soc. Rev.* 44 (2015) 4185–4191.
- [53] J. Cheng, X. Liang, Y. Cao, K. Guo, W. Wong, *Tetrahedron* 71 (2015) 5634–5639.
- [54] L.N. Neupane, J.M. Kim, C.R. Lohaniand, K.H. Lee, *J. Mater. Chem.* 22 (2012) 4003–4008.
- [55] M.H. Yang, P. Thirupathi, K.H. Lee, *Org. Lett.* 13 (2011) 5028–5031.
- [56] A. Dhir, V. Bhalla, M. Kumar, *Org. Lett.* 10 (2008) 4891–4894.
- [57] B. Gu, L. Huang, W. Su, X. Duan, H. Li, S. Yao, *Anal. Chim. Acta* 954 (2017) 97–104.
- [58] A.S. Rao, D. Kim, T. Wang, K.H. Kim, S. Hwang, K.H. Ahn, *Org. Lett.* 14 (2012) 2598–2601.
- [59] X. Cheng, Q. Li, J. Qin, Z. Li, *ACS Appl. Mater. Interfaces* 2 (2010) 1066–1072.
- [60] Y. Zhou, X. He, H. Chen, Y. Wang, S. Xiao, N. Zhang, D. Li, K. Zheng, *Sens. Actuators B Chem.* 247 (2017) 626–631.
- [61] Z. Ruan, Y. Shan, Y. Gong, C. Wang, F. Ye, Y. Qiu, Z. Liang, Z. Li, *J. Mater. Chem. C* 6 (2018) 773–780.
- [62] S. Yang, W. Yang, Q. Guo, T. Zhang, K. Wu, Y. Hu, *Tetrahedron* 70 (2014) 8914–8918.
- [63] A.S. Rao, D. Kim, T. Wang, K.H. Kim, S. Hwang, K.H. Ahn, *Org. Lett.* 14 (2012) 2598–2601.
- [64] Y.Q. Wu, X.Y. Wen, Z.F. Fan, *Spectrochim. Acta A* 223 (2019) 117315.
- [65] A. Gomathi, P. Viswanathamurthi, *Anal. Methods* 11 (2019) 2769–2777.
- [66] I.J. Chang, K.S. Hwang, S.K. Chang, *Dyes Pigments* 137 (2017) 69–74.
- [67] Y.Y. Gao, N. Yi, Z.Z. Qu, Z.Y. Li, T.T. Ma, H.D. Jia, W.L. Xing, G.Q. Yang, Y. Li, *Sens. Actuators B Chem.* 267 (2018) 136–144.